EuroDrying'2017 – 6th European Drying Conference
Liège, Belgium, 19-21 June 2017

# LABORATORY SCALE SPRAY DRYING OF ADVANCED MATERIALS FOR BATTERIES, LASERS AND BIOCERAMICS

C. Arpagaus[1], A. Collenberg[2], D. Rütti[2]

[1] NTB University of Applied Sciences of Technology Buchs, Institute for Energy Systems, Buchs, Switzerland
[2] BÜCHI Labortechnik AG, Flawil, Switzerland

E-mail of the corresponding author: ***cordin.arpagaus@ntb.ch***

*Abstract:* Spray drying technology is a suitable process applicable for large scale production of various advanced materials. Recent laboratory scale research focusses on the development of (1) nano/micro structured electrode materials for next generation lithium ion batteries with enhanced cell capacity and superior electrochemical performance, (2) transparent materials for laser ceramics, and (3) bioceramics, such as bone substitutes, dental implants and cements with improved bioactivity and therapeutic effects. This paper reviews the current research progress in these application fields and highlights the importance of laboratory scale spray drying in the corresponding advance materials processing routes.

*Keywords:* spray drying, advanced materials, batteries, transparent ceramics, bioceramics

## Introduction

Spray drying is widly applied as a processing step in the fields of material, chemical, food, and pharmaceutical industries. The method is continous, scalable, low cost, and provides the ability to generate functional powders with special structures, such as composite, core-shell, or encapsulated particles [1]–[3]. Spray drying is especially applied in the formation of composite particles and granules providing a better flowability in the filling and pressing steps. The particle morphology and size play an important role for the final material properties.

This paper reviews the current state of research on laboratory scale spray dried electrode materials for batteries, transparent ceramics for lasers, and bioceramics for bone tissue and dental cements applications (Figure 1). The article highlights the importance of spray drying as a intermediate synthesis step in the corresponding material processing routes.

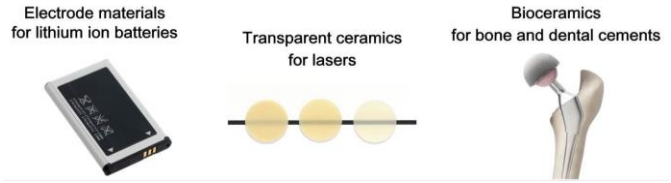


Figure 1: Spray drying applications reviewed in this study.

In this respect, the table-top equipments Mini Spray Dryer B-290 and Inert-Loop B-295 (Figure 2) are established and proven for spray drying water- and solvent-based solutions and suspensions into powders, granules, and composites with tunable particle size, shape, porosity, density, and chemical composition. The Inert Loop B-295 enables a fully closed system, which maximizes user safety and minimizes organic solvent wastage. In particular, laboratory scale spray drying allows processing of small amounts of powder ideal for feasibility studies in R&D and it provides data for further scale-up.

As an example, Figure 2 illustrates the spray drying process to form $Fe_2O_3$ nanoparticles into graphene oxide sheets ($Fe_2O_3$@GS) [3] as it is used for electrode material in battery applications. The mixed suspension (feed) is sprayed into fine droplets through the two-fluid nozzle by using compressed air or $N_2$. In the drying cylinder the solvent evaporates from the droplets and the particles solidify. The dried particles are separated from the drying gas in the cyclone and are recovered in a collection vessel.

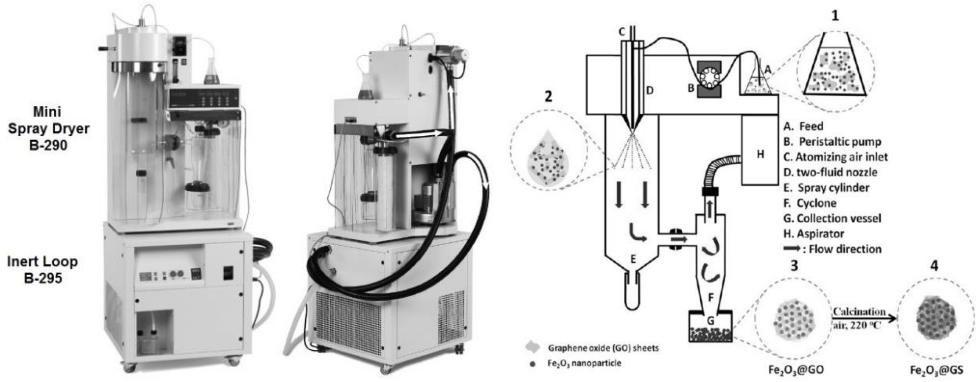


Figure 2: Mini Spray Dryer B-290 with Inert Loop B-295 (BUCHI Labortechnik AG) and schematic of spray drying of graphene-encapsulated $Fe_2O_3$ nanoparticles ($Fe_2O_3$@GS) [3].

## Spray dried electrode materials for battery applications

Besides high energy and power density, lithium ion batteries offer an excellent coulombic efficiency and low memory effect [4], [5]. Therefore, they are increasingly applied in electric vehicles, energy storage, portable electronics and power tools [6], [3]. Current research is directed towards new electrode materials [7]–[9] and synthesis procedures, i.e. solid state and wet chemistry methods [10], [11], that enables to push the boundaries of costs, energy and power density, cycle life, and safety [2]. General design strategies for performance enhancement are size reduction, formation of nano/micro composites, doping and functionalization, tuning particle morphology, and formation of coatings or shells around active materials [8].

Table 1. Procedures with spray drying for the synthesis of anode (LTO@GS [1], GS-Si [6], pSi/CNT/C [12], $Fe_2O_3$@GS [3]) and cathode materials (pPAN-S@GNS [2]).

| | | |
|---|---|---|
| 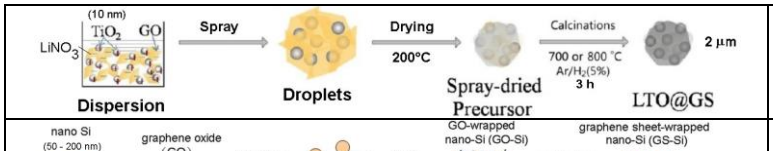  | Yuan et al. (2014) [1] | Anode materials |
| 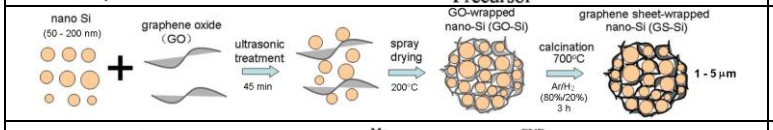  | He et al. (2011) [6] | |
| 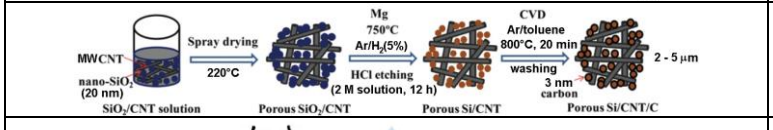  | Feng et al. (2014) [12] | |
| 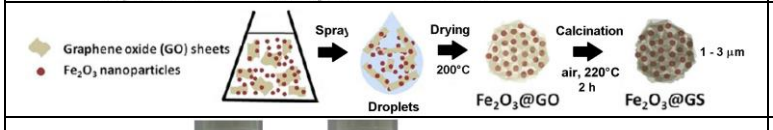  | Zhou et al. (2013) [3] | |
|   | Wang et al. (2014) [2] | Cathode material |

Table 1 illustrates some preparation procedures of graphene-wrapped composites where spray drying plays a crucial role as an intermediate fabrication step [1]–[3], [6]. First of all, a suspension of a nanopowder (e.g. $TiO_2/LiNO_3$ [1], polyacrylonitrile (PAN) [2], $Fe_2O_3$ [3], Si [6], $SiO_2$ [12]) with graphene oxide (GO) sheets [13] or carbon nanotubes (CNT) [12] is sonicated in water. Then, the mixed suspension will be spray dried. Composite particles with evenly dispersed nanoparticles embedded in graphene matrix with nano/micro structure of typically 1 to 5 µm size are formed. Finally, the obtained composites are further processed by thermal treatments, e.g. calcination [1], [3], [6], chemical reduction [13], or etching [12], while maintaining their particle morphology.

Table 2 provides further details about the conditions of sample prepartion, the laboratory scale spray drying parameters, and the further processing steps. Scanning electronic microscopy (SEM) images illustrate the morphology of the obtained spray dried composite particles. The actual research activities on spray dried electrode materials are particularly concentrated in China and the USA. Figure 3a shows the voltage profiles vs. Li/Li+ of such electrode materials. The corresponding cycling stability test results are depicted in Figure 3b.

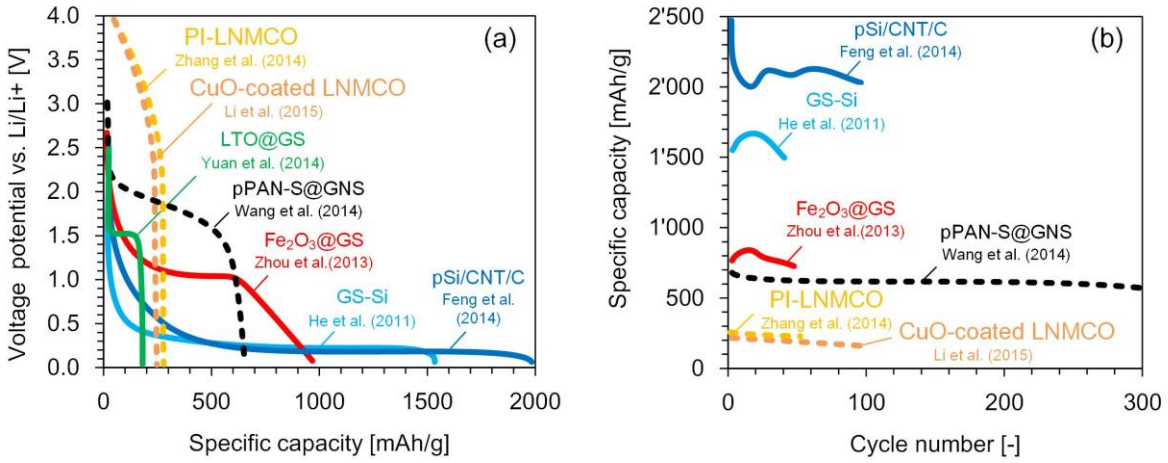


Figure 3: Voltage profiles (a) and cycle performances (b) of spray dried anode materials (solid lines, LTO@GS [1], $Fe_2O_3$@GS [3], GS-Si [6], pSi/CNT/C [12]) and cathode materials (dashed lines, PI-LNMCO [14], CuO-coated LNMCO [15], pPAN-S@GNS [2]).

Lithium-rich materials represented by $Li_{1.2}Mn_{0.54}Co_{0.13}Ni_{0.13}O_2$ (LNMCO) are promising candidates thanks to their high voltage and low cost [14]. An effective method to improve their cyclic stability is surface modification by coating. In this respect, CuO [15] or polyimide (PI) [14] coatings were applied to improve the electrochemical performance. Zhang et al. [14] successfully coated a thin PI layer (~3 nm) on the surface of LNMCO particles by using a polyamic acid (PAA) precursor solution followed by a thermal imidization process. The original LNMCO material was synthesized by spray drying and subsequent pyrolysis. The PI nanolayer remarkably enhanced the electrochemical performances of LNMCO. A fairly stable discharge capacity of 245 mAh/g with a retention to 91% after 50 cycles was achieved. The PI coating effectively separated the cathode material from the electrolyte and stabilized their interface at high voltage leading to a better cyclic performance.

Li et al. [15] prepared spherical cathode materials of CuO-coated LNMCO. Spray drying enabled the formation of a uniform powder with a homogeneously distributed CuO layer on the surface of the particles. The 2 wt% CuO-coated powders showed better cycling stability (174 mAh/g after 100 cycles) than non-coated LNMCO.

Table 2. Spray dried electrode materials for battery applications.

| Application, *reference* | Sample preparation, *spray drying conditions*, further processing steps | *Particle morphology*, electrochemical properties | |
|---|---|---|---|
| Anode material for Li-ion batteries<br><br>*He et al. (2011)* [6] | Nano-size Si (50-200 nm) sonicated for 45 min in aqueous graphene oxide (GO) suspension, *Mini Spray Dryer B-290, $T_{in}$ 200°C,* conversion of GO-Si to GS-Si composite in $H_2$/Ar at 700°C for 3 h | *1-5 µm compsites, nano-Si particles wrapped in graphene sheets,* high reversible charging capacity of 1'525 mAh/g, superior cycling stability | GS-Si 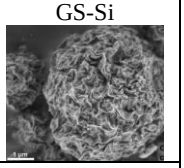 |
| Anode material for high power and large capacity Li-ion batteries<br><br>*Feng et al. (2014)* [12] | Aqueous suspension of nano-$SiO_2$ (20 nm) with multiwall carbon nanotubes (MWCNT), *Mini Spray Dryer B-290, nozzle cap 1.4 mm, $T_{in}$ 220°C, $T_{out}$ 120°C, feed rate 5 mL/min,* magnesio-thermic reduction at 750°C and HCl etching (2M solution, 12h) to convert pSiO2/CNT into pSi/CNT, CVD carbon coating to pSi/CNT/C | *2-5 µm spherical composites, porous, surface area 202 $m^2/g$,* reversible capacity about 2'100 mAh/g, excellent cycling stability | $pSiO_2$/CNT 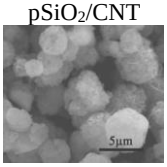 |
| Electric double-layer capacitors (EDLC)<br><br>*Qiu et al. (2015)* [13] | Aqueous suspension of graphene oxide (GO) dispersion (5 mg/mL), sonicated for 20 min, *Mini Spray Dryer B-190, spray cap 1.5 mm, $T_{in}$ 120°C, $T_{out}$ 80°C, aspirator 100%, feed rate 2.74 mL/min,* reduction of GO to r-GO in air at 225°C for 12 h | *1-2 µm r-GO particles, corrugated surface with alternating grooves and ridges, surface area 385 $m^2/g$,* specific capacitange 40 to 75 F/g | r-GO 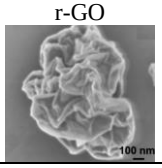 |
| Anode material for Li-ion batteries<br><br>*Zhou et al. (2013) [3]* | Nano-size $Fe_2O_3$ powder in aqueous GO suspension (1 mg/mL), weight ratio 8:2, *Mini Spray Dryer B-290, $T_{in}$ 200°C,* calcination in air at 220°C for 2 h to convert $Fe_2O_3$@GO into $Fe_2O_3$@GS | *1-3 µm particles, sphere-like, $Fe_2O_3$ nanoparticles uniformly embedded in GS matrix,* high reversible capacity of 711 mAh/g with a capacity retention of 94% after 50 cycles | $Fe_2O_3$@GS 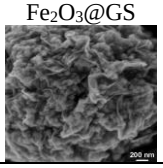 |
| Anode material for hybrid battery capacitor systems<br><br>*Yuan et al (2014) [1]* | Aqueous suspensions of GO, nano-$TiO_2$ (10 nm) and $LiNO_3$ (LTO:GO ratio 80:20), *Mini Spray Dryer B-290, $T_{in}$ 200°C,* calcination in Ar/$H_2$ (5%) at 700 or 800°C for 3h | *2 µm spherical GO-wrapped $TiO_2$ nanoparticles composites,* specific capacity of 174.4 mAh/g at 1 C with 1.93% GS, coulombic efficiencies ~100%, specific capacitance retains 90% of initial value after 20'000 cycles at 80 C | LTO@GS 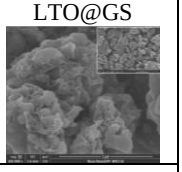 |
| Sulfur-based cathode materials for Li-ion batteries<br><br>*Wang et al. (2014) [2]* | Aqueous dispersion of polyacrylonitrile (PAN) particles (70 nm) and GS (PAN:GNS ratio 10:1), *Mini Spray Dryer B-290, Tin 220°C,* heat treatment of PAN@GNS at 300°C for 6 h in $N_2$ and sulfur to produce pPAN–S@GNS | *1-5 µm spherical nanoporous composites of pyrolyzed polyacrylonitrile-sulfur@graphene nanosheets (pPAN–S@GNS)* reversible capacity of 681.2 mAh/g, coulombic efficiencies ~100% after 300 cycles at 0.2 C rate | pPAN-S@GNS 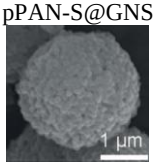 |
| Polyimide coated lithium-rich cathode material<br><br>*Zhang et al. (2014)* [14] | $Ni(CH_3COO)_2{\cdot}4H_2O$, $Co(CH_3COO)_2{\cdot}4H_2O$, $Mn(CH_3COO)_2{\cdot}$ $4H_2O$, and $LiCH_3COO{\cdot}2H_2O$ and citric acid in water (ratio 2:1) *Mini Spray Dryer B-290,* calcination at 400 °C for 6 h and at 900 °C for 12h to obtain $Li_{1.2}Mn_{0.54}Co_{0.13}Ni_{0.13}O_2$ (LNMCO), mixing and coating with polyamic acid (PAA) solution, treatment at 450°C to form PI-LNMCO | *Fine PI-LNMCO powders with a thin (~3 nm) PI coating,* stable discharge capacity of 245 mAh/g with a retention of 91% after 50 cycles | PI-LNMCO 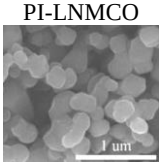 |
| CuO-coated LNMCO cthode materials for lithium ion batteries<br><br>*Li et al. (2015)* [15] | Aqeous suspension of 10 g $Li_{1.2}Mn_{0.54}Co_{0.13}Ni_{0.13}O_2$ particles (LNMCO, 200 nm) and 0.5 g $Cu(CH_3COO)_2{\cdot}H_2O$, *Mini Spray Dryer B-290,* heat treatment at 500°C in air for 4h | *2-5 µm spherical powder, 2 wt% CuO-coated LNMCO,* enhanced capacity compared to non-coated LNMCO, 174 mAh/g after 100 cycles | CuO-LNMCO 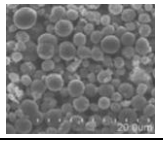 |

Hematite $Fe_2O_3$ has attracted much attention as intercalation electrode material because of its low processing cost and environmental friendliness [3]. $Fe_2O_3$@GS [3] composites obtained by spray drying showed significantly enhanced reversible capacity of 711 mAh/g compared to pristine $Fe_2O_3$ whose capacity strongly decreased with the cycling number.

The same research group at the Shanghai Jiao Tong University [1] successfully prepared spray dried lithium titanium oxide LTO@GS microspherical composites as anode materials for a hybrid battery/capacitor system. Anatase $TiO_2$ was used as starting material, which

offers great advantage in terms of large-scale industrial implementation. Under optimized conditions the battery delivered a specific capacity of 174 mAh/g. The specific capacitance still retained 90% of its initial value after 20'000 cycles at high charge/discharge rates.

Silicon based anode materials offer a large theoretical capacity ($Li_{15}Si_4$, 3'600 mAh/g) at moderate operating voltage (0.4 to 0.5 V vs. Li/Li+) [12]. On the other hand, the Li+ diffusion rate inside silicon is rather small [6] and the cycling stability limited because of the large volume change of Si (+270%) [8]. Nanonization and the addition of conducting graphene or carbon are effective ways of improving the electrochemical properties of Si-based materials. Inspired by this idea, He et al. [6] and Feng et al. [12] synthetisized composites of nano-Si-GS [6] and porous pSi/CNT/C [12] by using a spray drying step among other processes. The materials exhibited high reversible capacities of 1'525 mAh/g and 2'100 mAh/g respectively with superior cycling stability.

Sulfur with a theoretical capacity of 1'675 mAh/g is also a low cost and abundant element in the Earth's crust [8]. However, sulfur-based cathodes have a low electrical conductivity and suffer from about 80% volume change during cycling [2], [8]. This may destroy the electrical contact in standard carbon composite electrodes. Thus, Wang et al. [2] formed porous microparticles of pyrolyzed polyacrylonitrile-sulfur@graphene nanosheets (pPAN–S@GNS) by spray drying and subsequent heat treatment. The composites with nano/micro-structure provided a highly conducting network and enough voids to accommodate the volume change and facilitate Li-ion diffusion. The high reversible capacity of 681 mAh/g demonstrated great promise for application as a high-performance cathode in next-generation rechargeable lithium-sulfur batteries.

**Spray dried transparent ceramics for lasers**

Remarkable progress is also made in the production of laboratory scale spray dried ceramics for transparent solid-state lasers [16]–[19] and polycrystalline magnesium aluminate spinel ($MgAl_2O_4$) powders used as a refractory material for steel making [20].

In solid-state lasers, yttrium aluminium garnet (YAG, $Y_3Al_5O_{12}$) is commonly used as host material. Rare earth elements such as ytterbium (Yb), erbium (Er), praseodymium (Pr), or neodymium (Nd) are doped into YAG as active laser ions, which determine the light absorption and emission profiles. For example, Nd:YAG emitts infrared light at a wavelength of 1'064 nm and provides output power levels up to the kW range [19]. Yb:YAG lasers emit at 1'030 nm and are good substitutes for Nd:YAG in high-power applications. Er:YAG is lasing at 2'940 nm and couples well into water and body fluids making this laser especially useful for medicine and dentistry uses [21]. In comparison, Pr:YAG lasers offer intersting perspectives for applications in optics and photonics, e.g. in the field of scintillator materials, to count the energy and intensity of ionizing radiation [16].

In order to form transparent ceramics, the material must exhibit a very low concentration of defects and residual pores [18], [22]. The generation of spherical and soft granules by spray drying improves the homogeneous packing of these particles during pressing and provides high transmittance after reactive vacuum sintering.

Figure 4 illustrates the manufacturing process to produce transparent laser ceramics which includes a spray drying step. First, commercial oxide powders (e.g. $Al_2O_3$, $Y_2O_3$, $Yb_3O_3$, $Er_2O_3$, $Nd_2O_3$ or $Pr_6O_{11}$) are milled and suspended in water or ethanol.

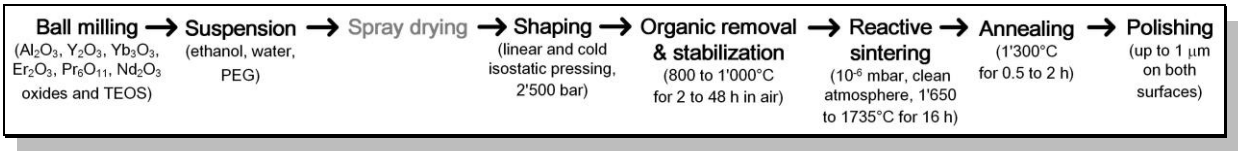


Figure 4: Manufacturing process for transparent laser ceramics.

Next, spray drying is applied to produce a soft granular powder with a size of about 2 to 10 μm. After shaping the powder by cold isostatic pressing and high temperature reactive sintering in a clean atmosphere under high vacuum [19], an optical grade polycrystalline laser ceramic is formed. The optical transparency depends mainly on the purity and the mean grain size of the used oxide powders.

Following this manufacturing process, Alderighi et al. [18] and Serantoni et al. [17] prepared transparent Yb:YAG ceramics, Cavalli et al. Er:YAG [21] and Pr:YAG [16] ceramics, and Esposito et al. [22] Nd:YAG laser materials.

Table 3 summarizes the experimental conditions of the suspension preparation and the spray drying process. SEM images of the spray dried powders and the polished ceramic surfaces illustrate the obtained particle morphologies and the microstructures of the surfaces.

Table 3. Spray dried transparent ceramic materials for lasers.

| Application, *references* | Sample preparation, *spray drying conditions* | *Particle morphology*, microstructure of polished ceramics surface, optical transparency |
|---|---|---|
| Yb:YAG laser ceramics<br><br>*Alderighi et al. (2010)* [18]<br>*Serantoni et al. (2012)* [17] | Suspension of $Al_2O_3$ (200 nm), $Y_2O_3$ (50 nm) and $Yb_3O_3$ (5.64 μm) oxides in ethanol with 0.5 wt% tetraethyl orthosilicate (TEOS) as sintering aid<br>*Mini Spray Dryer B-290 with Inert Loop B-295, spray nozzle 0.7 mm, solid concentration 16-24 wt%, feed rate 3 mL/h (5%), spray air 450 L/h and $N_2$ 473 L/h, aspirator rate 70 to 100% , $T_{in}$ 70°C, $T_{out}$ 50 °C* | *2 to 10 μm [18] and 8 to 14 μm [17] spherically shaped soft granules, process yield 30 g/h,*<br>ceramics with 80 to 90% transmittance at 1'100 nm<br> 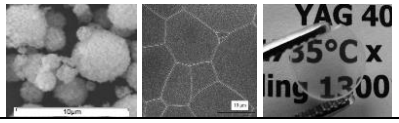 |
| Er,Yb:YAG laser ceramics<br><br>*Cavalli et al. (2013)* [21] | Aqueous suspension of $Al_2O_3$ (200 nm), $Y_2O_3$ (50 nm), $Er_2O_3$ (~20 μm) and $Yb_2O_3$ (5.64 μm) oxides with 1 wt% polyethylene glycol (PEG) 400 and 0.5 wt% TEOS<br><br>*Mini Spray Dryer B-290* | *2 to 15 μm spherical ready-to press powder,*<br>ceramics with pore-free microstructure after sintering, 10 to 30 μm grains, absense of defects,<br>78% transmittance at 1'100 nm<br> 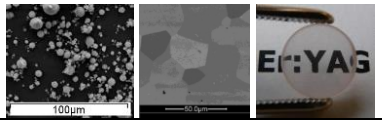 |
| Pr:YAG laser ceramics<br><br>*Cavalli et al. (2014)* [16] | Aqueous suspension of $Al_2O_3$ (200 nm), $Y_2O_3$ (50 nm) and $Pr_6O_{11}$ oxides with 1 wt% PEG 400 and 0.5 wt% TEOS<br><br>*Mini Spray Dryer B-290* | Regular crystalline microstructure with 20 to 60 μm grain size, clean grain boundaries,<br>80% transmittance at 1'100 nm<br> 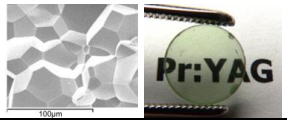 |
| Nd:YAG laser ceramics<br><br>*Esposito et al. (2011)* [22] | Suspension of $Al_2O_3$ (200 nm), $Y_2O_3$ (50 nm) and $Nd_2O_3$ (30-50 nm) oxides in ethanol with 1 wt% PEG 400 and 0.5 wt% TEOS<br>*Mini Spray Dryer B-290 with Inert Loop B-295, solid concentration 17 wt %, nozzle diameter 0.7 mm, feed rate 3 ml/min, spray air 450 L/h, aspirator rate 100%, $T_{in}$ 70°C* | *2 to 10 μm spherical granules,*<br>78% transmittance at 1'100 nm<br> 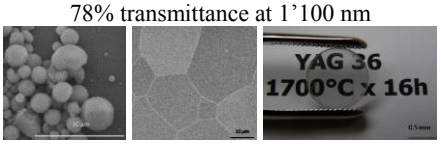 |
| Transparent $MgAl_2O_4$ spinel ceramics<br><br>*Ramavath et al. (2014)* [20] | Aqueous slurry of $MgAl_2O_4$ spinel powder (200 nm)<br><br>*Mini Spray Dryer 290 with Inert Loop B-295, solid concentration 68 to 70 wt%, feed rate 15 mL/min, $T_{in}$ 170°C, $T_{out}$ 140°C* | *5 to 15 μm spherical granules with smooth surface,*<br>30 to 50 μm grain size of sintered material $MgAl_2O_4$<br>80 to 85% transmittance between 400 and 800 nm,<br>80 to 87% transmittance between 3 and 5μm<br> 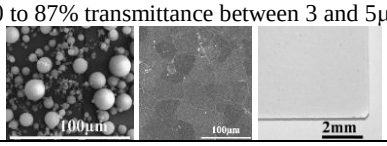 |

Spray drying suspensions of mixed nano-sized oxides has shown to be an excellent method for obtaining ready-to press granulated powders serving as YAG based laser ceramics [16]–[18], [21], [22] and transparent polycrystalline $MgAl_2O_4$ spinel powder [20]. The soft spray dried spherical granules guarantee a close and homogeneous particle packing during pressing. Consequently, the formation of a pore-free material after sintering [16] occurred with a high transmittance in the range of 80 to 90% at 1'100 nm wavelength comparable with

commercially available laser grade ceramic material [17], [22]. The achieved microstructures examined by SEM were found to be regular and fully crystalline formed by equiaxed grains of about 10 to 60 µm diameters with clean grain boundaries [21], [16]. The absence of defects is indirectly confirmed by the high transmittance.

Ramavath et al. [20] prepared spray dried $MgAl_2O_4$ granules providing high homogeneity and enhanced flow behaviour for the formation of transparent polycrystalline spinel ceramics by colloidal slip casting. The sintered ceramics exhibited uniform microstructure with 40 µm grain size. The optical transmittance reached 80 to 87%.

## Spray dried bioceramics for bone and dental cements

Another research focus is on spray dried bioceramics, i.e. bone graft materials and cements for dental implants. Table 4 shows a selection of spray dried bioceramics. In particular, the experimental conditions for the sample preparation and the spray drying are summarized. SEM photographs illustrate the structural morphologies of the obtained powders.

In bone tissue engineering, the bioceramic hydroxyapatite (HAp) is well known for its biocompatibility, non-toxicity, and bioactivity. It accounts for about 60 to 70% of the mineral phase in the human bones [23]. Spray drying is applied to convert hydroxyapatite slurries into fine powders as bone graft materials with adaptable porosity and particle size.

Lopez-Noriega et al. [24] encapsulated therapeutic pro-osteogenic peptides into polymer microparticles by spray drying and incorporated the received particles into porous collagen-hydroxyapatite scaffolds to assess their potential to enhance osteogenesis. Alginate, chitosan, gelatine, and poly(lactic-co-glycolic acid) were chosen as polymers for the encapsulation of the peptide. The composite scaffolds retained their interconnected porous structure and acted as reservoir for the controlled release of the active therapeutic peptide. The study demonstrated the potential to enhance bone tissue regeneration by these composite materials.

Table 4. Spray dried bioceramics as bone graft materials and cements for dental implants

| Application, *reference* | Sample preparation, *spray drying conditions* | *Particle morphology* | |
|---|---|---|---|
| Magnetic hyperthermia treatment of cancer<br><br>*Donadel et al. (2009)* [23] | Suspensions of iron oxide and hydroxyapatite (HAp)<br><br>*Mini Spray Dryer B-191 (former model of B-290), spray nozzle 0.7 mm, spray air 600 NL/h, feed rate 8 mL/min, aspirator 95%, $T_{in}$ 170°C, $T_{out}$ 90°C* | 0.5 to 12 µm spherical particles with core/shell structure | HAp-coated iron oxide<br> 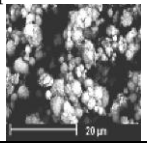 |
| Porous collagen-hydroxyapatite (CHA) scaffolds for bone tissue regeneration<br><br>*Lopez-Noriega et al. (2014)* [24] | 1 g polymer (alginate, chitosan, gelatine) in 200 mL water, peptide PTHrP 107-111:polymer ratio 25.2 mg:100 g (further fabrication: 100 mg microparticles in 1 mL water mixed with 9 mL CHA slurry)<br><br>*Mini Spray Dryer B-290, feed rate 15%, aspirator 80%,$T_{in}$ 140 to 160°C* | 1 to 10 µm particles, spherical shape with smooth surface, gelatine based materials with wrinkled texture | Peptide loaded polymer<br> 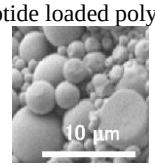 |
| Glass ionomer cements as dental restorative material<br><br>*Monmaturapoj et al. (2012)* [25] | Aqueous suspension of glass powders incoporating barium BaO and and magnesium MgO ions<br><br>*Mini Spray Dryer B-290* | 25 µm spherical shaped $ZrBa_2Mg_1$ particles with irregular structure | $ZrBa_2Mg_1$ glass powder<br> 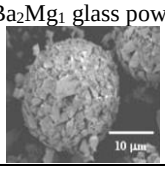 |
| Miserite glass-ceramics for dental implants<br><br>*Saadaldin et al. (2013)* [26] | Hydrolysis and polycondensation of metal alkoxides in aqueous solution<br>*Mini Spray Dryer B-190 (former model of B-290), feed rate 10 mL/min, $T_{in}$ 160°C, $T_{out}$ 80°C,* calcination at 200 to 700°C for 2 h in vacuum oven, melting at 1'150°C for 3 h and 1'250°C for 1 h in furnace, quenching in iced water | Spray dried powder calcinated and melted to transparent glass frits | no SEM picture available |

Magnetic iron oxide particles are increasingly used in medical diagnosis for magnetic resonance imaging and in cancer therapies involving targeted drug delivery and magnetic induction hyperthermia, a technique to destroy cancer cells. For this purpose, the magnetic particles need to be pre-coated with substances that assure biodegradability, stability, and non-physiological toxicity. Donadel et al. [23] coated magnetic iron oxide particles with hydroxyapatite by spray drying for the treatment of bone cancer and to promote bone formation. The results showed that spray drying is an efficient and inexpensive method for forming spherical particles with unique core/shell structure.

In dentistry, glass ionomer cements are used as dental restorative material for filling teeth and as luting cements. These cements are generated by an acid-base mixing reaction of glass powder and a co-polymer liquid. In this regard, Monmaturapoj et al. [25] incoporated alkaline earth metals (barium BaO and magnesium MgO ions) in the glass powder in order to improve the compressive strength of the glass ionomer cements. Spray drying aqueous suspensions of those glass powders was applied to form spherical shaped 25 µm sized particles with irregular structure. The glass powders have the potential to be used as teeth filling materials.

Machinable biomaterials allow dentists to design and fabricate customized dental restorations with a high level of accuracy and precision. In this respect, Saadaldin et al. [26] synthesized bioactive and machinable miserite glass-ceramics as a substitute for metallic dental implants made of titanium and zirconia. A combination of wet chemical synthesis using sol-gel chemistry, spray drying, calcination, melting, and quenching was applied to prepare a homogeneous transparent glass ceramic with good sintering, mechanical and optical properties, as well as excellent machinability. In vitro tests showed that the prepared miserite glass-ceramic is bioactive and supports the attachment and proliferation of osteoblast-like cells comparable to clinically proven titanium surfaces.

## Conclusions

Spray drying is recognized as a very efficient and simple one-step synthesis process for the formation of spherical shaped powders of defined size with tunable nano/micro composite morphologies.

In particular, spray drying is suitable for the industrial scale production of high-performance electrode materials with high specific capacity and cycling stability. Uniform composite powder are produced with evenly dispersed active nanoparticles embedded in conductive graphene matrix. The composites provide enough voids to accommodate the volume change of the active nanoparticles. Surface coatings are further applied to improve the electrochemical performance.

Spray drying of nano-sized oxide suspensions has shown to be an excellent method for the generation of ready-to-press granulated powders serving as transparent YAG-based laser ceramics. The spherical and soft granules enable a close and homogeneous packing during pressing and the formation of a pore-free and high transparent ceramic material after reactive sintering.

In bone tissue engineering, spray drying enables the formation of fine bioceramic powders as bone graft materials with adaptable porosity and particle size. Therapeutic molecules are encapsulated into polymers to enhance bioactivity and to control the release of the active therapeutic. Spray drying is also applied to prepare unique core/shell structures of hydroxyapatite coated magnetic iron oxide particles to treat bone cancer and to promote bone formation. For dental applications, the incorporation of alkaline earth metals in glass powders improves the compressive strength of glass ionomer cements.

## References

[1] T. Yuan, W.-T. Li, W. Zhang, Y. He, C. Zhang, X.-Z. Liao, and Z.-F. Ma, "One-Pot Spray-Dried Graphene Sheets-Encapsulated Nano-Li4Ti5O12 Microspheres for a Hybrid Batcap System," *Ind. Eng. Chem. Res.*, vol. 53, pp. 10849–10857, 2014.

[2] J. Wang, L. Yin, H. Jia, H. Yu, Y. He, J. Yang, and C. W. Monroe, "Hierarchical Sulfur-Based Cathode Materials with Long Cycle Life for Rechargeable Lithium Batteries," *CHEMSUSCHEM Full Pap.*, vol. 7, pp. 563–569, 2014.

[3] G. Zhou, J. Wang, P. Gao, X. Yang, Y. He, X. Liao, J. Yang, and Z. Ma, "Facile Spray Drying Route for the Three-Dimensional Graphene-Encapsulated Fe2O3 Nanoparticles for Lithium Ion Battery Anodes," *Ind. Eng. Chem. Res.*, vol. 52, pp. 1197–1204, 2013.

[4] B. J. Landi, M. J. Ganter, C. D. Cress, R. a. DiLeo, and R. P. Raffaelle, "Carbon nanotubes for lithium ion batteries," *Energy Environ. Sci.*, vol. 2, no. 6, p. 638, 2009.

[5] T. Sasaki, Y. Ukyo, P. Novák, and S. Information, "Memory effect in a lithium-ion battery," *Nat. Mater.*, vol. 12, pp. 569–575, 2013.

[6] Y.-S. He, P. Gao, J. Chen, X. Yang, X.-Z. Liao, and Z.-F. Ma, "A Novel Bath Lily-Like Graphene Sheets-Wrapped Nano-Si Composite as a High Performance Anode Material for Li-ion Batteries (Electronic Supplementary Information)," *RSC Adv.*, vol. 1, pp. 958–960, 2011.

[7] B. Dunn, H. Kamath, and J.-M. Tarascon, "Electrical Energy Storage for the Grid: A Battery of Choices," *Science (80-. ).*, vol. 334, no. 6058, pp. 928–935, 2011.

[8] N. Nitta, F. Wu, J. T. Lee, and G. Yushin, "Li-ion battery materials: Present and future," *Mater. Today*, vol. 18, no. 5, pp. 252–264, 2015.

[9] M. Winter, J. O. Besenhard, M. E. Spahr, and P. Novák, "Insertion Electrode Materials for Rechargeable Lithium Batteries," *Adv. Mater.*, vol. 10, no. 10, pp. 725–763, 1998.

[10] D. Jugović and D. Uskoković, "A review of recent developments in the synthesis procedures of lithium iron phosphate powders," *J. Power Sources*, vol. 190, no. 2, pp. 538–544, 2009.

[11] T. V. S. L. Satyavani, a. Srinivas Kumar, and P. S. V. Subba Rao, "Methods of synthesis and performance improvement of lithium iron phosphate for high rate Li-ion batteries: A review," *Eng. Sci. Technol. an Int. J.*, vol. 19, no. 1, pp. 178–188, 2015.

[12] X. Feng, J. Yang, Y. Bie, J. Wang, Y. Nuli, and W. Lu, "Nano/micro-structured Si/CNT/C composite from nano-SiO2 for high power lithium ion batteries," *Nanoscale*, 2014.

[13] H. Qiu, T. Bechtold, L. Le, and W. Y. Lee, "Evaporative assembly of graphene oxide for electric double-layer capacitor electrode application," *Powder Technol.*, vol. 270, pp. 192–196, 2015.

[14] J. Zhang, Q. Lu, J. Fang, J. Wang, J. Yang, and Y. Nuli, "Polyimide Encapsulated Lithium-Rich Cathode Material for High Voltage Lithium-Ion Battery," *ACS Appl. Mater. Interfaces*, vol. 6, pp. 17965–17973, 2014.

[15] B. Li, Y. Yu, and J. Zhao, "Facile synthesis of spherical xLi2MnO3 (1-x) Li(Mn0.33 Co0.33 Ni0.33)O2 as cathode materials for lithium-ion batteries with improved electrochemical performance," *J. Power Sources*, vol. 275, pp. 64–72, 2015.

[16] E. Cavalli, L. Esposito, M. Bettinelli, A. Speghini, K. V. Ivanovskikh, R. B. Hughes-Currie, and M. De Jong, "YAG:Pr3+ transparent ceramics for applications in photonics: synthesis and characterization," *Mater. Res. Express*, vol. 1, no. 45903, 2014.

[17] M. Serantoni, A. Piancastelli, A. L. Costa, and L. Esposito, "Improvements in the production of Yb:YAG transparent ceramic materials: Spray drying optimisation," *Opt. Mater. (Amst).*, vol. 34, pp. 995–1001, 2012.

[18] D. Alderighi, A. Pirri, G. Toci, M. Vannini, L. Esposito, A. L. Costa, A. Piancastelli, and M. Serantoni, "Characterization of Yb:YAG ceramics as laser media," *Opt. Mater. (Amst).*, vol. 33, pp. 205–210, 2010.

[19] J. Sanghera, W. Kim, G. Villalobos, B. Shaw, C. Baker, J. Frantz, B. Sadowski, and I. Aggarwal, "Ceramic laser materials: Past and present," *Opt. Mater. (Amst).*, vol. 35, no. 4, pp. 693–699, 2013.

[20] P. Ramavath, P. Biswas, K. Rajeswari, M. B. Suresh, R. Johnson, G. Padmanabham, C. S. Kumbhar, T. K. Chongdar, and N. M. Gokhale, "Optical and mechanical properties of compaction and slip cast processed transparent polycrystalline spinel ceramics," *Ceram. Int.*, vol. 40, pp. 5575–5581, 2014.

[21] E. Cavalli, L. Esposito, J. Hostaša, and M. Pedroni, "Synthesis and optical spectroscopy of transparent YAG ceramics activated with Er3+," *J. Eur. Ceram. Soc.*, vol. 33, pp. 1425–1434, 2013.

[22] L. Esposito, A. Piancastelli, A. L. Costa, M. Serantoni, G. Toci, and M. Vannini, "Experimental features affecting the transparency of YAG ceramics," *Opt. Mater. (Amst).*, vol. 33, pp. 713–721, 2011.

[23] K. Donadel, M. D. V. Felisberto, and M. C. M. Laranjeira, "Preparation and characterization of hydroxyapatite-coated iron oxide particles by spray-drying technique," *An. Acad. Bras. Cienc.*, vol. 81, no. 2, pp. 179–186, 2009.

[24] A. López-Noriega, E. Quinlan, N. Celikkin, and F. J. O'Brien, "Incorporation of polymeric microparticles into collagen-hydroxyapatite scaffolds for the delivery of a pro-osteogenic peptide for bone tissue engineering," *APL Mater.*, vol. 3, no. 1, pp. 1–9, 2015.

[25] N. Monmaturapoj, S. Kinmonta, W. Thepsuwan, S. Channasanon, and S. Tanodekaew, "Preparation and characterisation of glass ionomer cements incorporating barium and magnesium ions," *Adv. Appl. Ceram.*, vol. 111, no. 3, pp. 159–164, 2012.

[26] S. A. Saadaldin, S. J. Dixon, D. O. Costa, and A. S. Rizkalla, "Synthesis of bioactive and machinable miserite glass-ceramics for dental implant applications," *Dent. Mater.*, vol. 29, pp. 645–655, 2013.